Studies of Configuration Control Effects on Dynamic Behavior of Heliotron J Plasmas

Tohru Mizuuchi, Shinji Kobayashi, Satoshi Yamamoto[a], Hiroyuki Okada, Kazunobu Nagasaki, Gen Motojima[b], Shinya Watanabe[b], Hajime Arimoto[b], Kensuke Murai[b], Fumiyori Hamagami[b], Daisuke Katayama[b], Hironori Matsuoka[b], Akino Nakajima[b], Hiroshi Takahashi[b], Hiroyuki Yasuda[b], Kiyofumi Mukai[b], Akiyuki Matsuyama[b], Yusuke Kowada[b], Katsuyuki Hosaka[b], Shiori Mihara[b], Nobuhiro Nishino[c], Takashi Minami[d], Yousuke Nakashima[e], Yasuhiro Suzuki[d], Sadayoshi Murakami[f], Kiyomasa Watanabe[d], Masayuki Yokoyama[d], Yuji Nakamura[b], Kiyoshi Hanatani, Katsumi Kondo[b], Shoichi Okamura[d], Fumimichi Sano

Institute of Advanced Energy, Kyoto University, Gokasho, Uji 611-0011, Japan
[a]Kyoto University Pioneering research Unit for Next Generation, Gokasho, Uji 611-0011, Japan
[b]Graduate School of Energy Science, Kyoto University, Gokasho, Uji, 611-0011, Japan
[c]Graduate School of Engineering, Hiroshima University, Higashi-Hiroshima 739-8527, Japan
[d]National Institute for Fusion Science, 322-6 Oroshi-cho, Toki 509-5292, Japan
[e]Plasma Research Center, University of Tsukuba, Tsukuba, Ibaraki 305-8577, Japan
[f]Graduate school of Engineering, Kyoto university, Kyoto 606-8501, Japan

(Received day month year / Accepted day month year)

The transition to an improved confinement mode in NBI-only plasma is investigated in Heliotron J, focusing on the onset condition of the transition. The transition, identified by a drop in the Hα intensity and an increase in the stored energy, the line-averaged electron density, has been observed in the Co-injection case. The experiment shows (1) the delay time between the NBI turned-on and the drop of the Hα intensity decreases with the power, and (2) the transition occurs at a certain toroidal current (bootstrap current and NBCD current). The critical current depends on the vacuum rotational transform. The free-boundary equilibrium calculation predicts that the rotational transform and the shape of the magnetic surface, especially in the outer region, can be modified asymmetrically to the current direction.

Keywords: Heliotron J, rotational transform, effect of non-inductive plasma current, transition of confinement mode, NBI plasma

1. Introduction

Heliotron J [1, 2] is a low-magnetic-shear device with an L/M = 1/4 helical coil (R_0 = 1.2 m, $B_0 \leq$ 1.5 T) based on the helical-axis heliotron concept [3], where the bumpiness, ε_b, is introduced as a new control knob of field configuration in addition to the other major field harmonics, helicity and toroidicity. One of the major objectives of Heliotron J project is to examine the effects of the new field parameters on the plasma performance and to experimentally explore this advanced concept. The configuration control studies are essential parts of the Heliotron J experiment.

The study of ε_b-control effects on the bulk plasma confinement and behavior of fast-ions were initially performed for ECH plasmas selecting three different ε_b configurations with the same rotational transform at the last closed flux surface (LCFS), $\iota(a)/2\pi$ in the vacuum condition (i.e. no plasma effects) [4, 5]. As for the ε_b-effect on the fast-ion behavior, which was examined by superimposing an NBI or ICRF pulse on ECH target plasmas, the higher ε_b configuration is preferable for the confinement of low- and high-pitch angle fast-ions. These observations are qualitatively consistent with the drift optimization viewpoint. On the other hand, as for the global energy confinement, the dependence is not so simple and we have tried to understand the observations based on the discussion of the effective ripple modulation amplitude, ε_{eff}. The preliminary analysis suggests that the lower ε_{eff} configuration seems to be preferable for the global confinement for ECH-only plasma These experiments have expanded to NBI-only plasmas [6], where the difference of τ_E^{exp} in high- and medium-ε_b configurations is not clear compare to that for ECH-only plasma. These observations suggest the possibility of different ε_b-dependence of the global energy confinement time between ECH-only and NBI-only plasmas.

On the other hand, as experimentally demonstrated

author's e-mail: mizuuchi@iae.kyoto-u.ac.jp

in W7-AS [7] and Heliotron J [8], the value of the edge rotational transform $\iota(a)/2\pi$ is essential for the good plasma confinement in a low magnetic-shear device, including L-H transition and MHD activities. The effects of rational surfaces in the core region have been studied in many tokamaks and helical devices from the viewpoint of MHD activities. Recently the effects of low-order rational surfaces have been discussed from the viewpoint of the appearance of external/internal transport barriers or enhanced confinement modes in helical devices [9, 10]. In addition, the edge rotational transform is also closely related with the field topology for so-called a "built-in" divertor in heliotron/stellarator systems.

The initial study of rotational transform effects on the global confinement in Heliotron J were performed by for ECH-only plasma [11]. Since the transition to the improved confinement mode (H-mode) was discovered in Heliotron J, the accessibility condition to the transition has been experimentally investigated for different configurations labeled by the vacuum edge rotational transform $\iota(a)/2\pi|_{vac}$ [8]. ECH- and ECH+NBI experiments indicate the existence of $\iota(a)/2\pi|_{vac}$-windows for the high quality H-mode ($\tau_E^{exp}/(f\times\tau^{ISS04}) > 1.5$) close to the low-mode rational numbers of $\iota(a)/2\pi|_{vac}$. Here, τ^{ISS04} and f are the global energy confinement time by the international (inter-machine) stellarator scaling and a new configuration-descriptive re-normalization factor driven for each configuration subgroup of the experimental database, respectively [12, 13]. Figure 1 shows such $\iota(a)/2\pi|_{vac}$-dependence for ECH+NBI plasmas [8]. The

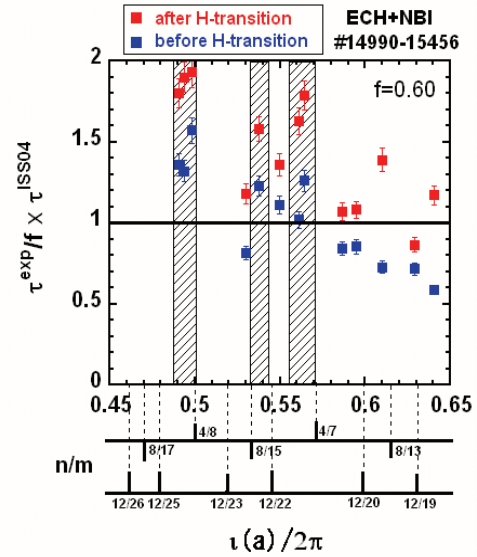

Fig. 1 Configuration effect on the normalized global energy confinement time of for ECH+NBI plasma. Each configuration is labeled by $\iota(a)/2\pi|_{vac}$. The window for the high quality H-mode (hatching zone) is observed close to the low-mode rational numbers of $\iota(a)/2\pi|_{vac}$ [8].

power and density thresholds of the H-mode are observed to depend on the configuration (i.e. $\iota(a)/2\pi|_{vac}$), but the systematic dependences between them are not fully understood. It might have to consider the influence of the topology ("shape") of the magnetic surfaces on the poloidal viscous damping rate, which influences the formation of the radial electric field through the plasma poloidal rotation [14]. The poloidal viscous damping rate depends also on the existence of the rational surface [15].

Even for non-Ohmic heating plasmas in a helical device, non-inductive plasma current can be driven by the pressure-gradient (bootstrap current), ECCD and NBCD. The modification of $\iota(r)/2\pi$ due to such non-inductive plasma current can create new rational surfaces in the core region. In the edge region, the change of the rotational transform can modify the divertor plasma distribution in a low-shear device. In the Heliotron J experiments, it is experimentally confirmed that the bootstrap current and ECCD can be controlled by the bumpiness tailoring [16]. A tangential NBI system [17] can also control the direction and intensity of NBCD current by selecting the beam lines and by controlling the injection power. Experimentally, the effects of the plasma current and its radial profile on the edge field topology and divertor plasma distribution have been investigated in Heliotron J from viewpoints of divertor control and balk plasma confinement [18]. An experimental detection of the rotational transform modification during a discharge has been tried in Heliotron J by using the sensitivity of MHD activities on the rational surfaces [19].

This paper reports recent experimental investigation into the effects of the non-inductive plasma current (or resultant modification of $\iota(r)/2\pi$) on the onset of the

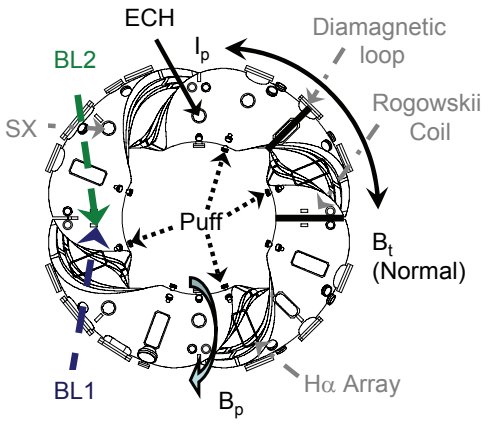

Fig.2 Top view of the Heliotron J device. In the case of the "normal" operation, the direction of the magnetic field is clockwise, where the toroidal current flowing in the counter-clockwise direction enhances the poloidal magnetic field strength. ("additive current")

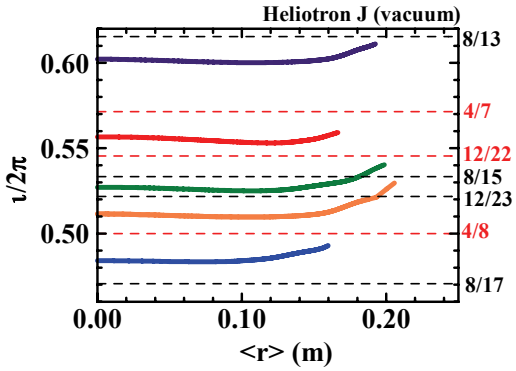

Fig. 3 Radial profile of the vacuum rotational transform for several configuration. The horizontal dashed lines indicate some low-mode rationals.

transition event.

2. Experimental setup

The details of the Heliotron J device is described in [1, 2]. Figure 2 schematically shows the top view of Heliotron J with the main heating and diagnostic systems. The initial plasma is produced by the 70GHz second harmonic X-mode ECH system launched from a top port located at the straight section of Heliotron J. The hydrogen neutral beam (30 keV, 0.7 MW/beam-line) is injected using two tangential beam-lines facing each other (BL1 and BL2). Selecting one of the beam-line or changing the direction of the confinement field, Co- or CTR-injection is performed. The working gas is hydrogen or deuterium.

The configuration of the confinement field is controlled using the five types of the external coils, the helical coil, two individual sets of the toroidal coils (TA and TB) and two sets of the vertical coils (AV and IV). The major part of the field configuration is determined by the helical and toroidal coil currents. The bumpiness is mainly controlled by changing the coil current ratio of TA and TB coils, I_{TA} and I_{TB}, respectively. Trimming of other coil currents, it is possible to control ε_b within tolerable change in the other major Fourier components of the confinement field (helicity and toroidicity), $\iota(a)/2\pi|_{vac}$, the plasma volume and the major radius [4]. On the other hand, $\iota(r)/2\pi|_{vac}$ can be controlled by mainly changing the current ratio of the helical coil to the toroidal coils. Here, it is possible to minimize the change of the bumpiness by keeping the current ratio of I_{TA}:I_{TB} to be constant. Some examples of radial profile of the rotational transform in the vacuum condition are shown in Fig. 3. The ε_b at ρ = 2/3 and $\iota(a)/2\pi|_{vac}$ for the standard (STD) configuration of Heliotron J are $\approx$ 0.06 (I_{TA}:I_{TB} = 5:2) and $\approx$ 0.56, respectively.

3. Numerical study of plasma current effects on the field configuration

A free-boundary equilibrium calculation is useful to obtain a prospect of the deformation of the configuration by plasma pressure and/or current, and to understand the experimental observations.

Figures 4 and 5 show an example of such calculation obtained by using HINT2 [20] for the STD configuration. Here, we assume rather peaked plasma pressure- and current-profiles: $\beta(s) = \beta_0\times(1-s)^2$ with β_0 = 0.5%, $j_p(s) = j_0\times(1-s)^2$, where s denotes toroidal flux corresponding to the square of the normalized minor radius (= ρ^2). In Fig. 4, "vacuum" means no plasma condition (i.e. β = 0 %, the

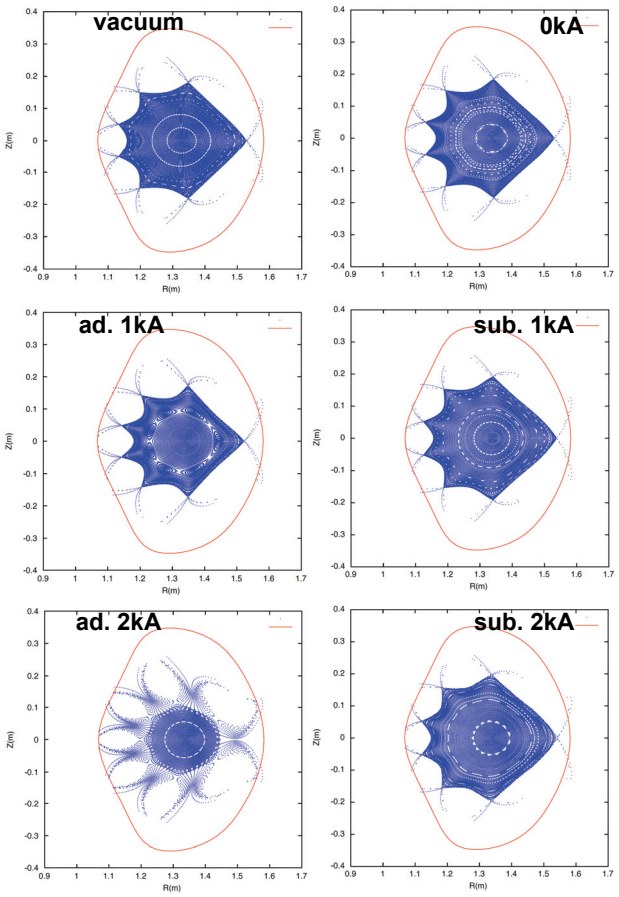

Fig.4. Effects of plasma pressure and current on the configuration.

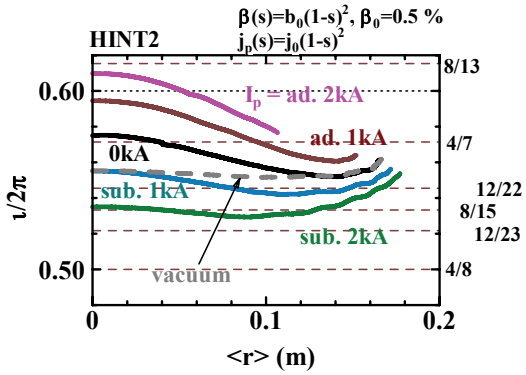

Fig.5. Effects of plasma pressure and current on the rotational transform.

net current I_p = 0 kA). The case of "additive current" direction (i.e. the current increases $\iota/2\pi|_{vac}$) is indicated as "ad. *kA" and the opposite case is "sub. *kA" in the figure. Figure 5 shows the effects on the rotational transform obtained by the same calculations for Fig. 4. As shown in Figs. 4 and 5, the plasma current can modify not only the rotational transform but also the "shape" of the last closed flux surface. Moreover, as discussed in [18], even for the same net-current value, the difference in current profile j(s) has important effects on the modification. It should be noted that the effects are not symmetry to the net current direction. The effect of the plasma pressure can be somewhat compensated by the subtractive current. Moreover, the "proximity" to the rational number, 4/7 for the STD configuration, is important since the low-mode resonance has an important role on the field topology,. The vacuum rotational transform at the edge is about 0.56 (i.e. less than the rational number 4/7) in the standard configuration, $\iota(a)/2\pi$ become close to the rational by the additive current, but the subtractive current increase the distance from the resonance condition.

4. Transition in NBI-only plasma

In this study, we focus on the NBI-only plasmas to simplify the situation and to take advantage of current controllability of NBCD in the density region higher than the empirical critical (lower-limit) density for the transition [8].

Figure 6 shows an example of the time traces for the stored energy, line-averaged density and Hα intensity from an NBI-only plasma in the STD configuration, where the direction of the confinement field is the normal direction and the working gas is hydrogen. The plasma initiation was performed by using a short pulse (~ 6ms) of the 70GHz 2X ECH microwaves. After that, the plasma was heated and sustained by Co-NBI (BL2, P_{inj} ~ 0.46 MW/28kV). Here, "Co-"means the NBCD current increases the vacuum rotational transform ("additive" current). At t ~ 206 ms, a sudden drop of Hα intensity and increases of the stored energy and line-averaged density were observed, indicating the onset of transition to an improved confinement mode. The changes in the radial profile of SX-intensity and the ion saturation current in the scrape-off region (not shown) indicate that this phenomenon is an edge relating event. The Hα intensity was rapidly increased from ~ 220 ms, and finally the back transition occurred followed by the decrease of the stored energy. It is interesting to note that there is some time delay between the start of NBI and the drop of the Hα intensity. This delay time is longer than the "build-up time" of NBI-only plasma (~16 ms (from t ~186 to t ~102 ms) in this particular shot).

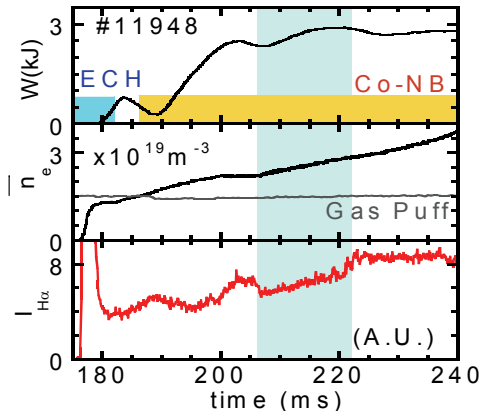

Fig.6. Typical example of NBI-only plasma showing the transition. Time trace of the stored energy (top), the line-averaged density (middle) and the intensity of Hα (bottom) are plotted.

As shown in the previous section, the toroidal current and plasma pressure (<β> ~ 0.2 % in this shot) can modify the rotational transform profile and the shape of LCFS.

4.1. Differences between Co- and CRT-NBI

The Co- and CTR-NBI plasmas are compared in the same vacuum configuration with $\iota(a)/2\pi|_{vac} \approx 0.54$ [21], where a natural resonance of m/n = 15/8 exists at $\rho \approx 0.87$ in vacuum. Figure 7 shows the time traces of some plasma parameters for CO- and CTR-NBI plasmas. In this experiment, only the beam-line of BL1 was injected into D^+ plasma initiated by ECH. By changing the field direction, Co- and CTR-injections were examined. The port-through NB powers (P_{inj}) are 0.58 and 0.56 MW for Co- and CTR-injection cases, respectively. Although the evaluation of the absorption efficiency of CTR-injection NBI is an on-going task, the stored energy and the line-averaged density for the both discharges have similar

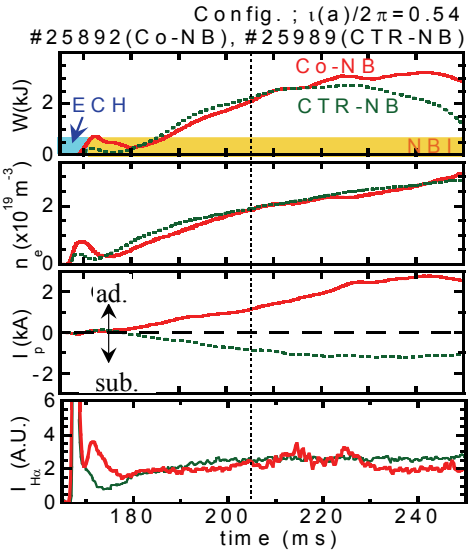

Fig.7. Comparison of Co- (red) and CTR-NBI (green) plasmas in the same vacuum configuration.

values, respectively, at least for the time interval of 200 ms < t < 220 ms. The direction of the plasma current is consistent with the expectation from the NBCD scenario but the intensity is not the same for the both discharges. Since the bootstrap current I_{BS} always flows to the additive direction in this configuration, NBCD current in the CTR-NBI case is somewhat compensated by I_{BS}. This cancellation effect usually becomes large in higher density (or stored energy) range since I_{BS} is an increasing function of the pressure gradient.

As shown in Fig. 7, the decrease in the Hα intensity and increase in the growth rate of the stored energy are observed in the Co-NBI case, but no clear change in Ha intensity or change in the "growth rate" of the stored energy were observed in the CTR-NBI case. In other configurations with different $\iota(a)/2\pi|_{vac}$ or the bumpiness, the transition event has not been observed for CTR NBI-only plasma in the range of P_{inj} ~ 0.25-0.6 MW.

In the Co-NBI case, the changes in Hα and the stored energy were observed at three timing (t ~ 204, 214 and 225 ms), indicating repetitive L-H-L sequences in this discharge. In next subsection, we will discuss the delay time between the start of NBI and the onset timing of the transition (determined by the drop of Hα intensity), we focus on the first event since for later event it is not so easy to control the density by gas-puffing.

4.2. Heating power dependence of the delay time

The delay time between the start of NBI and the drop of the Hα intensity was investigated by changing the heating power for two vacuum configurations with ε_b = 0.06 (medium ε_b) and 0.15 (high ε_b), where $\iota(a)/2\pi|_{vac}$ was set at almost the same value of 0.56. The experiment was performed under the reversed field direction with the beam-line BL1 (Co-injection for this field direction). Since the density was controlled in the range of $1.5–2.0\times10^{19}$ m^{-3} in this experiment, the absorption efficiency of NBI is considered to be almost the same (~ 30%) for the both configurations. This density range is higher than the empirical critical (lower-limit) density for the transition obtained from the previous experiments. The similar NBI-only plasma experiment was also performed for the vacuum configuration with ε_b = 0.01 (low ε_b) and $\iota(a)/2\pi|_{vac} \approx 0.56$. However no clear transition event was observed for the low-ε_b configuration even in the same experimental conditions of the injection power and the plasma density. It should be noted that for ECH+NBI plasmas, the transition was rather easily observed in the previous experiment although the improvement factor was low compared to that for the medium-ε_b case [4].

Figure 8(a) shows the delay time Δt as a function of P_{inj} for the high- and medium-ε_b configurations. The delay time for each configuration is almost the same value and depends on the injected power; Δt ~ 20 ms at P_{inj} ~ 0.6 MW,

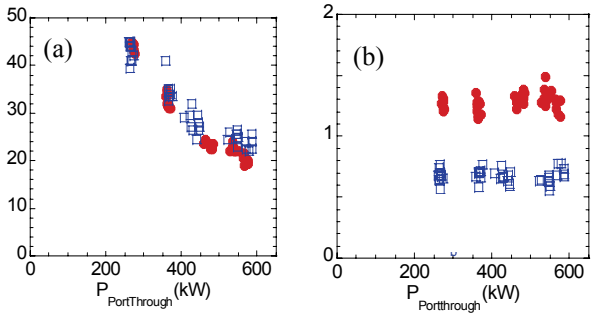

Fig.8. Power dependences of the delay time (a) and the plasma current at the onset timing of the transition (b) for high (red) and medium (blue) bumpiness configuration.

and it elongates to Δt ~ 40 ms at ~ 0.3 MW.

From the viewpoint of the configuration effect on the transition, it is interesting to check the value of the plasma current at the onset timing of the transition event since the plasma current modifies the field configuration as shown in Section 3. Figure 8(b) shows the toroidal current at the onset timing as a function of P_{inj}. It is clearly shown that the transition happens when the toroidal current reaches a critical I_p value which depends on the configuration; 0.7±0.1kA for the medium-ε_b 1.3±0.2kA for the high-ε_b configurations, respectively.

4.3. Configuration effects on the critical current

The effects of the plasma current on the field configuration should depend on the vacuum rotational transform. In order to investigate the effect of $\iota(a)/2\pi|_{vac}$ on the critical current discussed in the previous subsection, the $\iota(a)/2\pi|_{vac}$-scan experiment was performed for NBI-only plasma by changing the coil current ratio of the helical coil to the toroidal coils with the fixed I_{TA}:I_{TB} ratio. (I_{TA}:I_{TB} = 5:2, medium-ε_b). Figure 9 shows the toroidal current at the onset timing as a function of

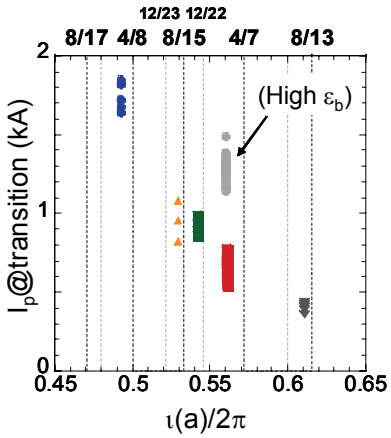

Fig.9. $\iota(a)/2\pi|_{vac}$-dependence of the critical toroidal current for the transition in NBI-only plasmas. Major low-mode rational numbers are also indicated.

$\iota(a)/2\pi|_{vac}$. The density and NBI power range are the same as that for Fig. 8 in this experiment, and the data from Fig. 8(b) for the high-ε_b case is also plotted as a reference. Although we tried Co- and CTR-injection experiments in the same configurations, no transition has been observed in the CTR-injection NBI-only plasmas under the present experimental conditions and selected $\iota(a)/2\pi|_{vac}$-values. Therefore, the plots in Fig. 9 are all additive current data. As shown in the figure, the critical current exists for all configurations and its value systematically decreases as increase of $\iota(a)/2\pi|_{vac}$.

5. Discussions

Under the present experimental condition (P_{inj} and magnetic configuration), no transition has been observed in the CTR-injection NBI-only plasmas. The P_{inj}-scan experiment shows the power dependence of the delay time after the NBI turned-on to the onset of the transition. This might indicate that the effective heating power P_{heat} was too low for the CTR-injection to make the transition. However, it is natural to consider that P_{heat} is not so different between Co- and CTR-cases since almost the same stored energy as that in Co- NBI plasma was obtained in the CTR-NBI plasma (Fig. 7).

In this study, we found out the existence of the critical current for the onset of the transition. In the CTR-injection case, since the current direction of NBCD is opposite to that of the bootstrap current, the total current becomes lower than that in Co- injection case and the current profile would be different. The free-boundary equilibrium calculation predicts that the rotational transform and the shape of the magnetic surface can be modified asymmetrically to the current direction (Fig. 4). As shown in Fig. 9, the examined values of $\iota(a)/2\pi|_{vac}$ in this study were located at smaller side of the nearest low-mode rational number. Therefore, roughly speaking, the additive current increase the edge rotational transform and approach to the low-mode rational number, but the subtractive current has the opposite effect. It is not easy to directly explain the $\iota(a)/2\pi|_{vac}$–dependence of the critical current by this simple idea, but the rational near the plasma edge would have some important effect on the transition event. Similar power dependence of delay time for ETB event is reported [22] in a high shear device, CHS. Here the delay time decreases as getting close $\iota(a)/2\pi|_{vac}$ to 1.

6. Summary

The transition to an improved confinement mode in NBI-only plasma is investigated in Heliotron J, focusing on the onset condition of the transition. In this study, we found out the existence of the critical current for the onset of the transition in NBI-only plasma. This critical current depends on the vacuum field configuration, $\iota(a)/2\pi|_{vac}$ and the bumpiness, but is independent of P_{inj}.

As for the H-mode in tokamaks, the effects of plasma rotation are discussed. We should take care of the effect of different momentum input direction from Co- and CTR-NBI. In order to obtain the toroidal/poloidal rotation velocity, we are preparing the diagnostic system of the charge exchange recombination spectroscopy.

Acknowledgments

The authors are grateful to the Heliotron J supporting group for their excellent arrangement of the experiments. They would also like to acknowledge Profs. T. Fukuda, T. Isobe, T. Mutoh, C. Suzuki, Y. Takeiri, N. Tamura, E. Ascasibar, B. Blackwell, C. Hidalgo, Q. Yang, B. Zurro for valuable discussions. This work is performed with the support and under the auspices of the Collaboration Program of the Laboratory for Complex Energy Processes, IAE, Kyoto University and Kyoto University 21st century COE Program “Establishment of COE on Sustainable Energy System”, the NIFS Collaborative Research Program (NIFS04KUHL001-005, NIFS05KUHL007, NIFS06KUHL007, NIFS06KUHL 009-010, NIFS06KUHL011, NIFS06KUHL 014-015) as well as and the Formation of International Network for Scientific Collaborations..

References

[1] F. Sano, et al., J. Plasma Fusion Res. **Ser.3**, 26 (2000) 26.
[2] T. Obiki, et al., Nucl. Fusion **41**, 833 (2001).
[3] M. Wakatani, et al., Nucl. Fusion **40**, 569 (2000).
[4] T. Mizuuchi, et al. Fusion Sci. Tech. **50**, 352 (2006).
[5] H. Okada, et al., Fusion Sci. Tech. **50**, 287 (2006).
[6] S. Kobayashi, et al., in the 2nd Joint Meeting of US-Jpn WS and Kyoto Univ. 21st COE Sympo. on "New approach in Plasma Confine. Exp. in Helical Systems", (Auburn, 2006).
[7] Wagner F, et al., 19th IAEA Fusion Energy Conference (Lyon, France, 2002) (Vienna: IAEA), OV2-4
[8] Sano F, et al., Nucl. Fusion **45**, 1557 (2005).
[9] F. Castejon, et al., Nucl. Fusion **44**, 593 (2004).
[10] K. Ida, et al., Nucl. Fusion **44**, 290 (2004).
[11] T. Obiki, et al., J. Plasma Fusion Res. **Ser.3**, 288 (2002).
[12] H. Yamada et al., Nucl. Fusion **45,** 1684 (2005).
[13] A. Dinklage et al., Fusion Sci. Tech. **51**, 1 (2007)
[14] F. Sano et al., Fusion Sci. Tech. **46**, 288 (2004)
[15] M. Hirsh, et al., Plasma Phys. Control. Fusion **42**, A231 (2000).
[16] G. Motojima, et al., Nucl. Fusion **46**, (2007).
[17] S. Kobayashi, et al., 20th IAEA Fusion Conf. (Vilamoura, Portugal, 2004) (Vienna: IAEA), EX/P4-41
[18] T. Mizuuchi, et al., Nucl. Fusion **47**, 395 (2007).
[19] G. Motojima, et al., P2-046 in this conference.
[20] Y. Suzuki, et al., Nucl. Fusion **46**, L19 (2006).
[21] S. Kobayashi, et al., in the 11th IAEA Tech. Meeting on H-mode Phys. Transport Barriers (Tsukuba, 2007).
[22] S. Okamura, et al., Nucl. Fusion **45**, 863 (2005).